*Sensors & Transducers, Vol. 243, Issue 4, August 2020, pp. 31-41*

www.sensorsportal.com

**Sensors & Transducers**

Published by IFSA Publishing, S. L., 2020
http://www.sensorsportal.com

# The Sensitivity of PolyPyrrole NanoTube / (Ag NanoParticle, Ag- NiO nanocomposite) Against $H_2S$ Toxic Gas at Low Temperature

**[1, *] Mohammed I. Hasan, [2] Isam M. Ibrahim and [1] Nabeel A. Bakr**

[1] Department of Physics, College of Science, University of Diyala, 10053, Iraq
[2] Department of Physics, College of Science, University of Baghdad, 10071, Iraq
[1] Tel.: 07718303912
E-mail: mohmadehsanehsan@gmail.com

*Received: 1 July 2020 /Accepted: 3 August 2020 /Published: 11 August 2020*

**Abstract:** In this study, polypyrrole nanotubes (PPy NTs) as $H_2S$ gas sensors were fabricated at room temperature, and report the effect of oxidant- to- monomer (O/M) molar ratio and (Ag nanoparticles, Ag-NiO nanocomposite) adding on the $H_2S$ gas sensing behavior, where the nanoparticles covered the nanotubes and some agglomeration was observed. The structure of the nanotubes was proved using field emission scanning electron microscopy (FESEM). X-ray diffraction (XRD) and energy dispersive X-ray spectroscopy (EDS) showed the compositions of all materials that exist in the prepared nanostructures. $H_2S$ gas sensing of PPy NTs for each molar ratio tested. It was found that the $H_2S$ gas sensing enhanced with an increase in the oxidant concentration. The response of $H_2S$ gas of the PPy NTs changed by (Ag) and (Ag-NiO) nanocomposite adding. It was observed that the largest response of $H_2S$ gas was 30.57 at 25 °C operating temperature, the response time and recovery time were 48.7 seconds and 10.7 seconds.

**Keywords:** Conducting polymer, Polypyrrole nanotube, $H_2S$ gas sensor.

## 1. Introduction

Polypyrrole (PPy) is one of the several conducting polymers that have been successful in getting attention due to their unique properties that is good thermal stability, high electrical conductivity, and easy route of synthesis, with many applications in the research of electronic devices just as supercapacitors, energy storage, batteries and sensors [1]. Polymerization of pyrrole occurs in the presence of ferric chloride used as an oxidizing agent [2]. Microtubes or nanotubes of PPy have been obtained by two methods: template-directed method and template-free growth method [3], and template-free growth has been developed in recent times to manufacture conducting polymer nanotubes by the soft template method [4]. The chemical synthesis of polypyrrole nanotubes (PPy NTs) in the presence of methyl orange represents a special type of template-free growth, which represents a soft template method [5]. The increase in the $FeCl_3$/Py molar ratio improved the conductivity of PPy NTs [6], so it is important to study the effects of the oxidant- to-monomer molar ratio on the physical properties of PPy NTs and their applications such as gas responsivity. $H_2S$ gas detection is important in many fields such as auto ventilation units and oil exploration [7]. Most of the gas sensors are fabricated from inorganic metal oxides such as $Fe_2O_3$, $WO_3$, and NiO, the disadvantages of metal oxide sensors represent that they cannot be operated only at high temperatures from

300 to 500 °C [8]. The amount of oxygen adsorption in nickel oxide is higher than other metal oxides used as gas sensors, which is related to the increase in electrical conductivity [9]. The performance of nickel oxide gas sensors toward $H_2S$ was enhanced by the combination (NiO) with noble metals [10]. The combination of silver with nickel oxide particles in PPy can enhance the doping level [11].

This work focused on the synthesis of PPy NTs in three different oxidant- to- monomer (O/M) molar ratios, and composite each (O/M) molar ratio with (Ag) nanoparticles by the chemical reduction method, and with (Ag-NiO) nanocomposite. PPy NTs, PPy NTs/ Ag nanoparticles, PPy NTs/ (Ag-NiO) nanocomposite were investigated by FESEM, X-ray diffraction, and EDS. The PPy NTs optical analysis was studied. the response of the gas of PPy NTs, PPyNTs/Ag nanoparticles, PPy NTs/(Ag-NiO) nanocomposite was studied to detect gaseous $H_2S$.

## 2. Material

The pyrrole monomer (Py) was obtained from Sigma Aldrich, England. Iron (III) chloride ($FeCl_3$), methyl orange (MO), and silver nitrate ($AgNO_3$) were purchased from Merck, Germany.

## 3. Methods

### 3.1. Preparation of Polypyrrole Nanotubes (PPy NTs)

PPy NTs were prepared by chemical polymerization of the pyrrole monomer with iron (III) chloride in distilled water in the presence of methyl orange. 1 ml of pyrrole with molarity (14 mM) mixed with (2.5 mM) methyl orange and dissolved in 288 ml of distilled water to form a (Pyrrole- Methyl orange) solution, and cooled at 5°C. (10 mM) iron (III) chloride dissolved in 33 ml distilled water and added drop wise to (Pyrrole- Methyl orange) solution over 2 h, as described before with (14 mM), and (25 mM) concentration of the iron (III) chloride, which were assigned by M1, M2, and M3, as shown in Table 1. After that, the reaction solutions were stirred for 24 h, then the PPy NTs precursor was separated by filtration and washed with acetone to remove the remaining methyl orange. Finally, the precursor was washed with ethanol and distilled water several times and dried at 80 °C for 6 h. After the precursor had derided, PPy NTs powder was obtained. (10 mg) of PPy NTs powder from each molar ratio was dissolved in 10 ml distilled water, and ultrasonicated for 45 min to form uniform PPy NTs solutions.

### 3.2. Preparation PPy NTs/ Ag Nanoparticles

(30 mg) of PPy NTs powder from each molar ratio added to (0.1 M) of the silver nitrate aqueous solution, and stirred for 24h to interact. The precipitate was filtered, washed with distilled water, and dried at 80°C, then PPy NTs/ Ag nanoparticles powder were obtained, which was assigned by M4, M5, and M6, as shown in Table 2. (10 mg) of PPy NTs/Ag nanoparticles powder dissolved in 10 ml distilled water, and ultrasonicated for 45 min to form uniform PPy NTs/ Ag nanoparticles solutions.

**Table. 1.** Represent the (MO: Py: $FeCl_3$) mM and molar ratio of the PPy NTs samples.

| Samples | MO | Py | $FeCl_3$ | MO: Py: $FeCl_3$ |
|---|---|---|---|---|
| M1 | 2.5 | 14 | 10.5 | 1: 5.6: 4.2 |
| M2 | 2.5 | 14 | 14 | 1: 5.6: 5.6 |
| M3 | 2.5 | 14 | 25 | 1: 5.6: 10 |

**Table 2.** (PPy NTs, PPy NTs/Ag nanoparticles, PPy NTs/ Ag-NiO nanocomposite) samples.

| Samples | PPyNTs | Ag nanoparticles | Ag- NiO nanocomposite |
|---|---|---|---|
| M1 | Pure | - | - |
| M2 | | | |
| M3 | | | |
| M4 | M1 | Ag nanoparticles | - |
| M5 | M2 | Ag nanoparticles | |
| M6 | M3 | Ag nanoparticles | |
| M7 | 5 mg M1 | - | 5 mg |
| M8 | 5 mg M2 | | 5 mg |
| M9 | 5 mg M3 | | 5 mg |

### 3.3. Preparation (Ag-NiO) Nanocomposite

(1 mM, 2.5 mM) of $AgNO_3$, $Ni(NO_3)_2.6H_2O$ was dissolved in (15 ml, 30 ml) of distilled water respectively, before (0.15 g) of CTAB, and (20 mM) of urea was added and the mixture was transferred into a 100 ml autoclave, which was closed and kept at 110 °C for 15 h. After that, the autoclave was cooled to room temperature by putting into an icy water bath, the precipitate was filtered and washed with methanol and distilled water several times and dried at 80 °C for 10h. The precipitate was calcined at 450 °C for 3 h [11].

### 3.4. Preparation (PPy NTs/ Ag-NiO) Nanohybrid Composite

(5 mg) powder of (Ag-NiO) nanocomposite was dissolved in 5 ml of distilled water, and (5 mg) powder of PPyNTs from each molar ratio dissolved in 5 ml of distilled water. These solutions were mixed and ultra-sonicated for 45 min to form uniform PPy NTs/(Ag-NiO) nanocomposite solutions, which were assigned by M7, M8, and M9, as shown in Table 2.

Finally, the above solutions were deposited drop by drop on p-type silicon (111) wafer substrates by using the spin coating technique by rotating the substrate at a speed of approximately1000–1500 RPM for 1 min in order to spread these solutions by centrifugal force.

### 3.5. Fabrication of $H_2S$ Gas Sensor

The $H_2S$ gas sensor device was fabricated as shown in Fig. 1. The above solutions were spin-coated on the p-type silicon substrate and molten gold was sprayed on the sample films after choosing a suitable mask to make the gold track to the electrode. The size of the gas sensor device was (1 cm × 1 cm). These devices were used to test the $H_2S$ gas sensing properties.

## 4. Results and Discussion

### 4.1. Field Emission Scanning Electron Microscope (FESEM)

The FESEM images of PPy are shown in Fig. 2. a, b, c. From M1 images, which were approximately 95 nm and 530 nm in diameter, the M2 diameters were (75, 100) nm, and the diameters of M3 were (40, 117) nm. Figs. 3 shows FESEM images of the M4, M5, and M6. The average diameter of the nanoparticle was approximately 60 nm represent in Fig. 3. a, b. Fig. 3. c, d shows nanoparticles aggregates as a globular or cluster, aggregates of nanoparticles founded on the outer surface of PPy NTs. FESEM images of the M7, M8, and M9 are shown in Fig. 4. a, b, c. Aggregates of nanocomposites observed on the outer surface of PPyNTs.

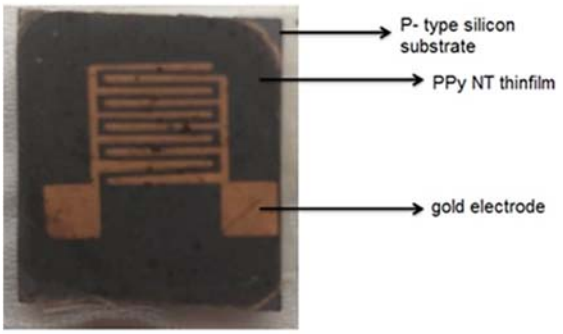


**Fig. 1.** $H_2S$ gas sensor was fabricated.

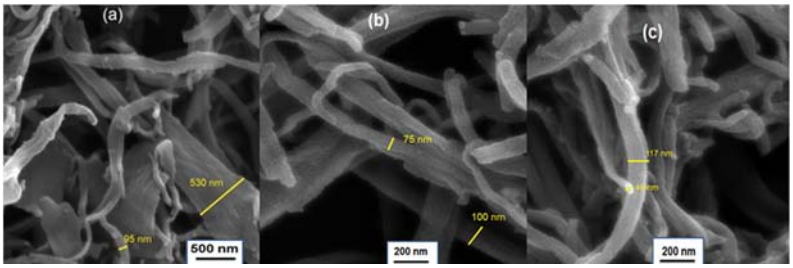


**Fig. 2.** FESEM images of (a) M1, (b) M2, and (c) M3.

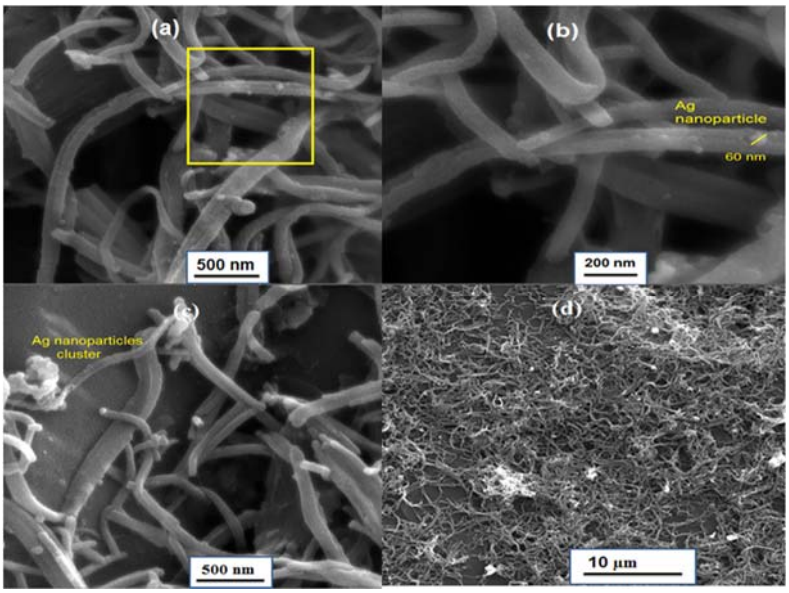


**Fig. 3.** FESEM images of (a), (b) M4, (c) M5, (d) M6.

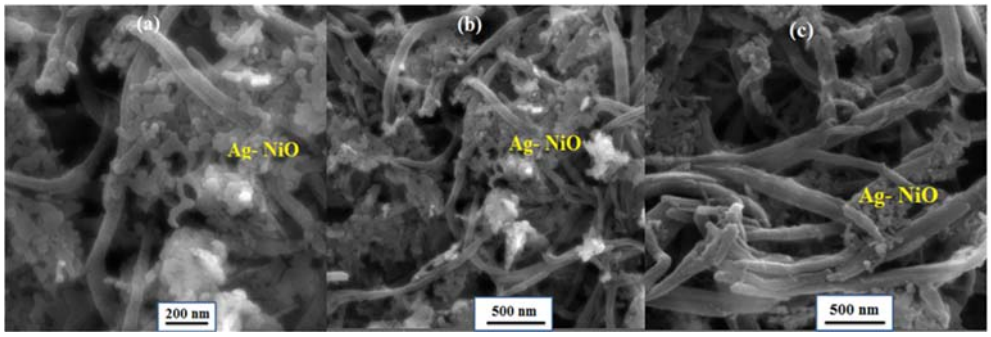


**Fig. 4.** FESEM images of (a) M7, (b) M8, and (c) M9.

## 4.2. X-Ray Diffraction (XRD)

As mentioned before, the solutions were spin-coated on p-type silicon substrate. The XRD patterns of the thin films are shown in Fig. 5. The XRD pattern of the M1 and M3 thin film shows amorphous peaks at 14.9°, 25.95°, 26.92°, and 25.77°, 26.6°, respectively. From the curve fitting of M1, the assumption that the narrow peak at 14.9° indicated to some crystallinity regions in the structure of PPy NTs. For the M4, M5, and M6 thin film, the diffraction peak at 38.18°, 38.22°, and 38.24° was assigned to the (111) reflection of Ag nanoparticle. The XRD of the pure (Ag- NiO) nanocomposite thin film shows peaks at 31.5°, 37.54°, 43.68°, and 63.89°. The diffraction peaks at 37.54°, 43.68°, and 63.8° were assigned to the (111), (200) and (220) reflections of the pure (Ag- NiO) nanocomposite [12]. The diffraction peaks of the M7, M8, and M9 thin film were (31.16°, 37.25°, 43.28°, 64.45°), (31.18°, 37.28°, 43.3°, 64.46°), and (31.2°, 37.3°, 43.32°, 64.48°) respectively.

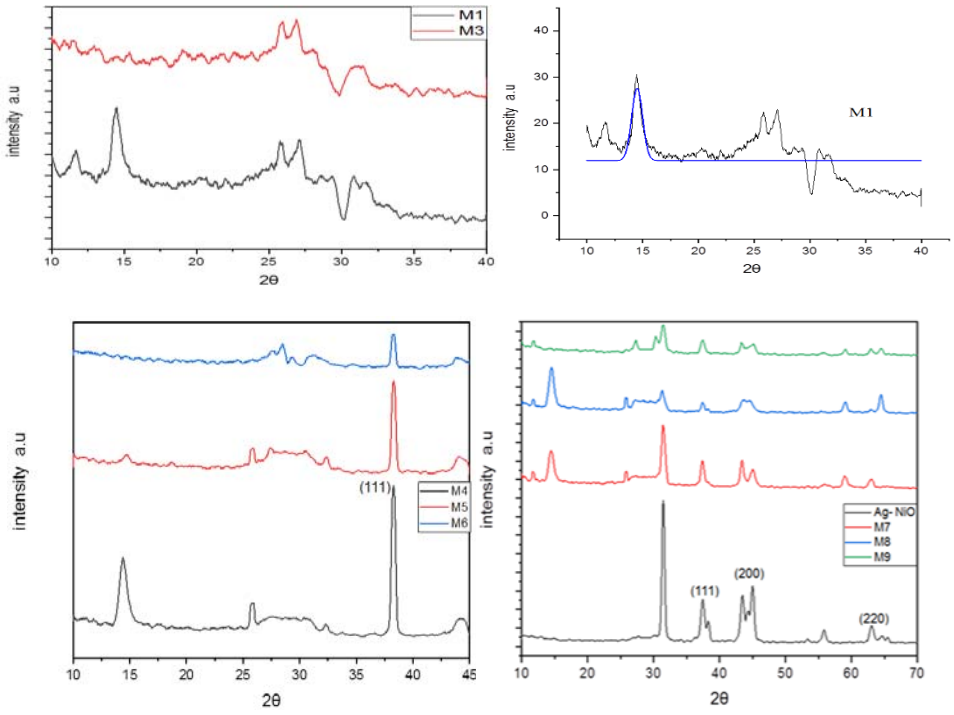


**Fig. 5.** XRD patterns of M1, M3, M4, M5, M6, pure Ag-NiO, M7, M8, and M9.

## 4.3 Energy dispersive X-ray spectroscopy analysis

Table 3 shows the EDS analysis of the samples. According to EDS analysis from the Fig. 6, (M1, M2, and M3) precursors composed of C (65 %, 55.18 %, 68.7 %), N (0 %, 17.26 %, 1.6 %), O (32.5 %, 26.9 %, 29.7 %), and Fe (2.5 %, 0.66 %, 0 %), respectively, these results indicate the PPy NTs structure, another word, M1, M2 prepared with (MO:Py:$FeCl_3$ ~ 1:5.6:4.2, 1:5.6:5.6) molar ratio, respectively. $FeCl_3$ may be a failure to capture all MO molecules because of the low oxidant concentration in the reaction solution so that some MO molecules do not take part in the complex $FeCl_3$-MO template, and the reaction between pyrrole monomers and $Fe^{+3}$ cations

associated with those MO molecules that did not participate in the complex $FeCl_3$- MO template structure and the pyrrole polymerization was occurred on the surface of the template [13]. Thus, very little degradation of the template occurs during pyrrole polymerization, leading to a non-hollow PPy NTs structure, M3 prepared with (MO:Py:$FeCl_3$ ~ 1:5.6:10) molar ratio, $FeCl_3$ may capture most MO molecules to form a complex $FeCl_3$- MO template structure because of the high oxidant concentration in the reaction solution. At the same time, a high value for the pyrrole monomer/ MO molar ratio ensures that the pyrrole monomer molecules diffuse into the template aggregation [13], so full degradation of the complex $FeCl_3$- MO template was occurred. After that, no template aggregation remained inside PPy NTs, leading to a hollow PPy NTs structure. This mechanism was related to the low weight percentage of the iron in EDS analysis for M3.

(M4, M5, and M6) composed of C (44 %, 48.6 %, 42.7 %), N (25.1 %, 25.8 %, 24.8 %), O (24 %, 22.1 %, 26.6 %), Fe (0.9 %, 0.2 %, 0 %), and Ag (6.1 %, 3.3 %, 5.8 %), respectively, these results indicate the PPy NTs/ Ag nanoparticles structure. (M7, M8, and M9) composed of C (38.8 % 31,2 %, 35.65 %), N (3.2 %, 8.0 %, 9.0 %), O (22.1 %, 19.8 %, 17.9 %), Fe (3.2 %, 0.8 %, 0 %), Ag (10.0 %, 10.9 %, 13.0 %), Ni (22.7 %, 29.3 %, 24.5 %), respectively, these results indicate the PPy NTs/ (Ag-NiO) nanocomposite structure.

**Table 3.** Show the EDS analysis of samples.

| Samples | Wt % | | | | | |
|---|---|---|---|---|---|---|
| | C | N | O | Fe | Ag | Ni |
| M1 | 65.0 | 0.00 | 32.5 | 2.5 | - | - |
| M2 | 55.18 | 17.26 | 26.9 | 0.66 | - | - |
| M3 | 68.68 | 1.59 | 29.73 | 0.00 | - | - |
| M4 | 43.98 | 25.09 | 23.96 | 0.88 | 6.10 | - |
| M5 | 48.65 | 25.79 | 22.12 | 0.19 | 3.25 | - |
| M6 | 42.67 | 24.8 | 26.70 | 0.00 | 5.80 | - |
| M7 | 38.81 | 3.16 | 22.09 | 3.21 | 10.0 | 22.73 |
| M8 | 31.21 | 7.96 | 19.78 | 0.83 | 10.88 | 29.34 |
| M9 | 35.65 | 9.02 | 17.94 | 0.00 | 13.0 | 24.5 |

### 4.4. Optical Analysis of PPy NTs

PPy showed three theoretical optical wavelengths, one at 345 nm corresponding to the π→π* band transition and the others at 450 nm and 877 nm, which are assigned to polaron and bipolaron band transitions [14]. Fig. 7 represents the absorbance spectra of PPy NTs recorded over the range (200–1100) nm. M1 sample showed three peaks at 296 nm, 465 nm and 930 nm respectively, which may be assigned to π→π*, polaron and bipolaron band transitions, M2 and M3 samples showed two peaks at 290 nm and 460 nm, which may be assigned to π→π* and polaron band transitions.

### 4.5. $H_2S$ Gas Sensor

The interaction between PPy and gas was strong at room temperature, so when PPy was contacted with gas, electron transferring between them can cause the change of the doping level, and the electrical conductance of the PPy, and hence changed in the electrical resistance of the sensing material [15]. Such a process occurred when PPy films exposed to $H_2S$ redox gas, the whole process represented by the following reaction:

$$PPyH^+ + H_2S \longrightarrow PPyH^+ \bullet H_2S$$

$$PPyH^+ \bullet H_2S \xrightarrow{\text{Moist Air}} PPyH^+ + H_2S + H_3O^+$$

The electrical resistance was measured as the output data, so ohmmeter enough to collect this data [16]. The response of the gas value (R %) was measured using the equation:

$$\mathbf{R\ \%} = | R_{gas} - R_{air} | / R_{air} \times 100\ \%, \quad (1)$$

where $R_{gas}$ is the electrical resistances of the sensor in $H_2S$ gas, and $R_{air}$ is the electrical resistance of the sensor in the air, and ΔR= Rgas- Rair, response time was the time taken for the gas sensor to get 90 % of maximum change in resistance on exposure to $H_2S$ gas, recovery time was the time taken by the sensor to get back 90 % of the initial resistance [17].

According to the chemical reduction process of silver nitrate by PPy NTs salt, part of silver ions present as silver chloride due to chloride ions originating from the $FeCl_3$ oxidant [18]. The exposure of PPy to the metal ion in an acid solution causes the PPy to be rapidly reportonation during ion reduced, when PPy immerged to silver nitrate aqueous solution, chemical interaction between them may be caused reportonation of PPy, and silver nitrate reduced with PPy to metallic silver as shown in Fig. 8 [19- 20].

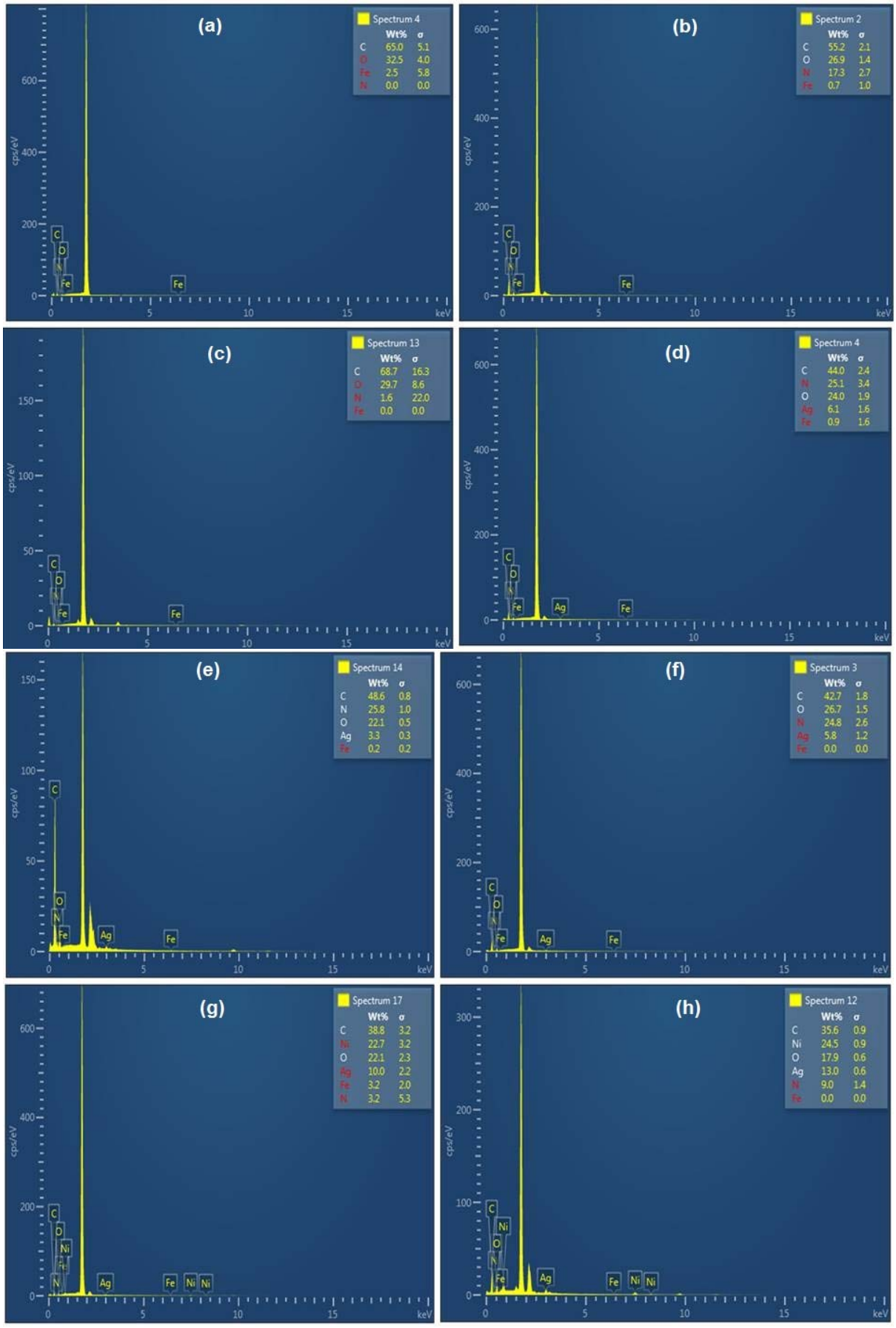


**Fig. 6.** EDS spectra of the a) M1, b) M2, c) M3, d) M4, e) M5, f) M6, g) M7, and h) M9.

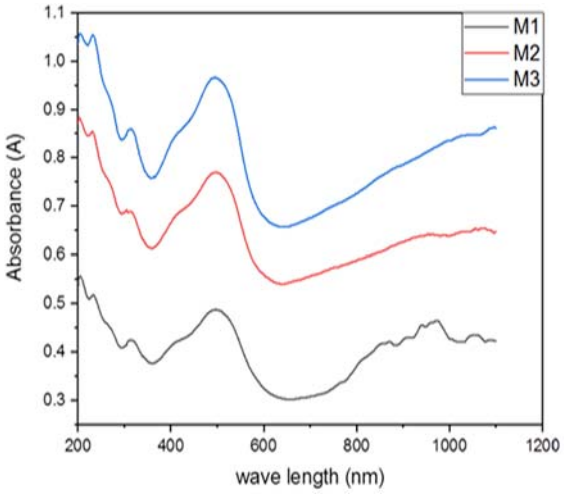


**Fig. 7.** UV- VIS absorbance spectra of PPy NTs samples.

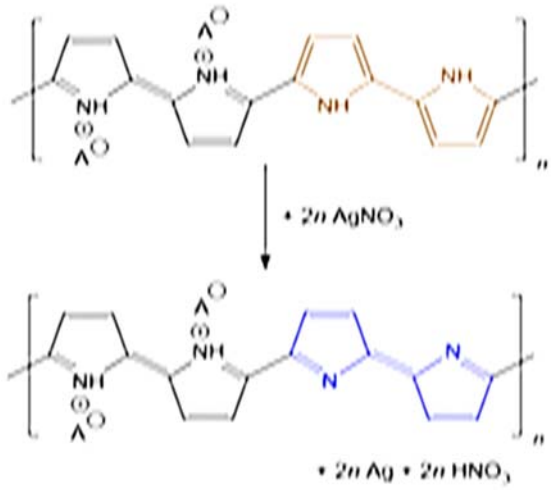


**Fig. 8.** Silver nitrate reduced with PPy to metallic silver [20].

$H_2S$ gas removed the electron from the aromatic ring of the PPy [21], As mentioned before, Pyrrole monomer was polymerized on the outer surface of the non-hollow PPy NTs structure [13], so after exposure to $H_2S$ gas, charge transfer across PPy backbone maybe influenced (attracting or repulsion) by $Fe^{+3}$ cations of the $Fe^{+3}$- MO aggregation was located inside PPy NTs, so $Fe^{+3}$ cation maybe obstructed the movement of this charge, resulting in an increase in the electrical resistance, and shown as a variety in the electrical resistance of M1, M2 as a function of time in Fig. 9, a, b. But $H_2S$ gas increased conductivity of PPy [22], so when the full degradation occurred, the exposure to $H_2S$ gas will enhance the conductivity of the hollow PPy NTs, leading to a decrease in the electrical resistance, and shown as a variety in the electrical resistance of M3 as a function of time in Fig. 9, c.

As mentioned before, the silver nanoparticles were combined with PPy NTs may be divided into two types: one silver ions composite with non- hollow PPy NTs as silver chloride, and other as a silver metallic when reprotonation of PPy chain by silver nitrate.

After exposure to $H_2S$, gas molecules were cleaved by the silver nanoparticles and act as catalysts, as silver has a high affinity for $H_2S$ gas, the $H_2S$ molecules were adsorbed on the (Ag) nanoparticles surface [23]. The dissociation of $H_2S$ gas molecules can occur, and these molecules change the charge carrier concentration of PPy [22] and electrical resistivity, shown as a variety in the electrical resistance of M4, M5, and M6 as a function of time in Fig. 9, d, e and f. The electrical resistivity of the PPy NTs were changed by the (Ag-NiO) nanocomposite adding, as shown in Fig. 9, g, h, and i.

Table 4 represents the responsivity, response time, and recovery time of the samples as $H_2S$ gas sensor devices at 25°C with 20 ppm gas concentration. Fig. 10 shows the response and recovery curves, and the response time of the samples. The responsivity of PPy NTs was increased when the value of the O/M molar ratio increased, as shown in Fig. 10 a. For PPy NTs/ Ag nanoparticles, the responsivity and the response time were decreased when the value of the O/M molar ratio increased, as shown in Fig. 10 b. The responsivity and response time of the non- hollow PPy NTs increased by (Ag-NiO) nanocomposite adding, but the responsivity and response time of the hollow PPy NTs decreased by (Ag-NiO) adding, as shown in Fig. 10 c.

**Table 4.** Represents the responsivity, response time and recovery time.

| Samples | Responsivity % | Response time S | Recovery time S |
|---|---|---|---|
| M1 | 0.51 | 32.4 | 23.4 |
| M2 | 1.05 | 14.2 | 9.5 |
| M3 | 10.8 | 86.9 | 27.2 |
| M4 | 30.57 | 48.7 | 10.7 |
| M5 | 12.2 | 45.3 | 13 |
| M6 | 0.6 | 37.8 | 8.1 |
| M7 | 2.8 | 47.7 | 67.4 |
| M8 | 1.16 | 37.2 | 33.4 |
| M9 | 7.48 | 76.5 | 31.9 |

Reproducibility of the samples upon periodic exposure to 20 ppm $H_2S$ gas at room temperature shown in Fig. 11. It was observed from Fig. 11 that the responsivity recovered to its original state, demonstrating that the samples have good repeatability toward $H_2S$ gas during the cycle test. Fig. 12 shows the sensors sense to 20 ppm $H_2S$ gas for 3 days, exhibiting quite good stability.

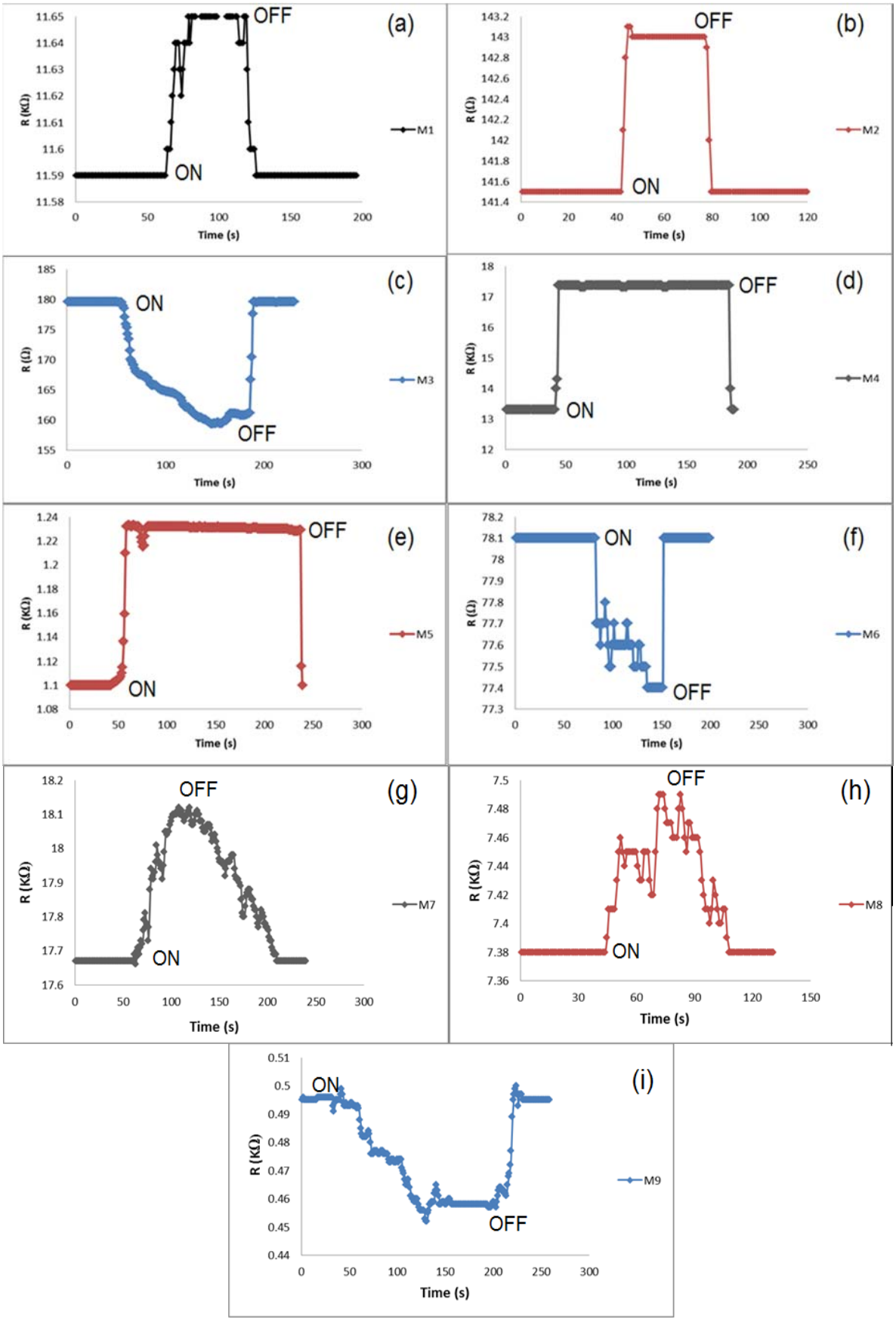


**Fig. 9.** Change in the electrical resistance of the samples with respect to time on the exposure of $H_2S$ gas at room temperature.

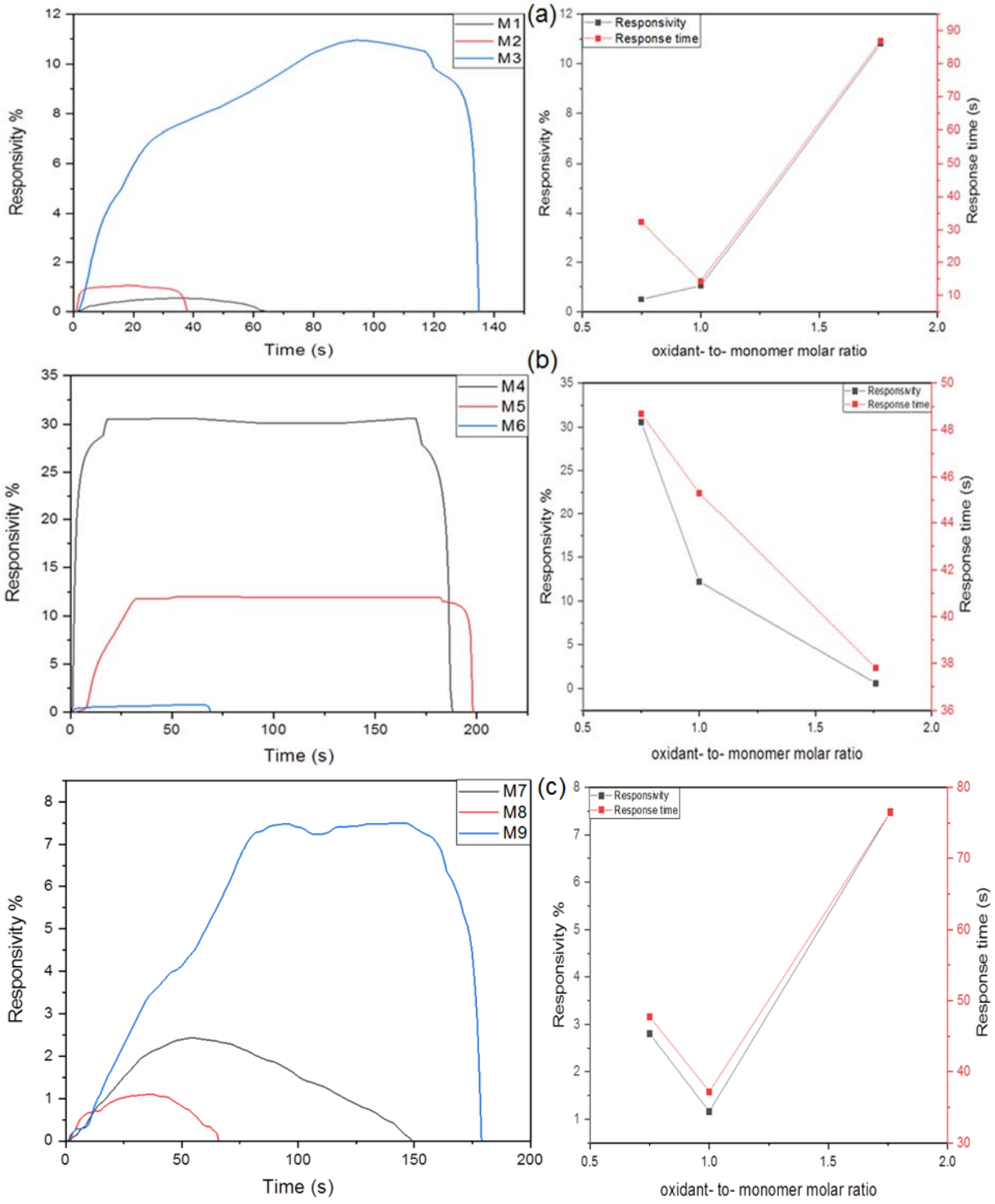


**Fig. 10.** a) Response and recovery curves, and response time of pure PPy NTs, b) Response and recovery curves, and response time of PPy NTs/Ag nanoparticles, d) Response and recovery curves, and response time of PPy NTs/Ag-NiO nanocomposite.

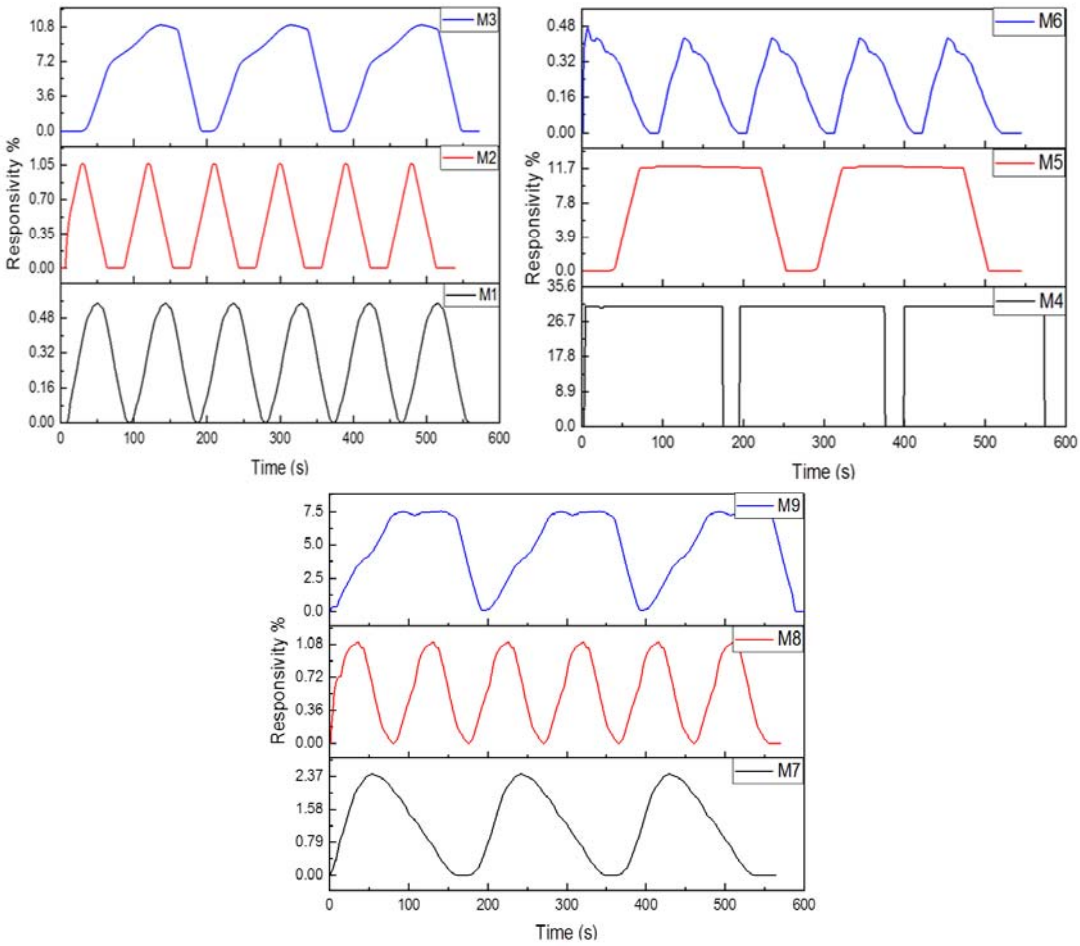


**Fig. 11.** The repeatability curve of samples sensor exposed to 20 ppm $H_2S$ at room temperature.

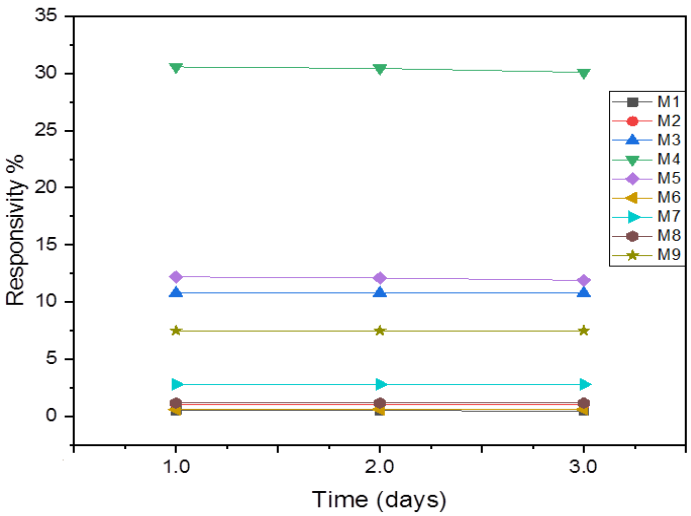


**Fig. 12.** The stability of the samples sensor upon exposure to 20 ppm $H_2S$ at room temperature.

## 5. Conclusion

Polypyrrole nanotubes (PPy NTs) with different diameters were synthesized by the soft template method. It was found that the $FeCl_3$-MO template degradation of PPy NTs affected by an increase in the $FeCl_3$ oxidant concentration. The responsivity of PPy NTs was changed and the high response of gas was obtained for the high oxidant concentration. The responsivity of the non-hollow PPy NTs structure was enhanced by chemically reducing silver ions from an aqueous solution of silver nitrate. The responsivity of PPy NTs was changed by (Ag-NiO) nanocomposite adding.

## References


[1]. T. Bashir et al., Magnetic, Electrical and Thermal Studies of Polypyrrole-Fe2O3 Nanocomposites, *Polym. Sci. - Ser. A,* Vol. 59, No. 6, 2017, pp. 902–908.

[2]. Y. M. Huang, F. fang Zhou, Y. Deng, and B. Gai Zhai, Effects of salt 9,10-anthraquinone-2-sulfonic acid sodium on the conductivity of polypyrrole, *Solid State Ionics,* Vol. 179, No. 27–32, 2008, pp. 1305–1309.

[3]. G. Li and Z. Zhang, Synthesis of Dendritic Polyaniline Nanofibers in a Surfactant Gel, *Macromolecules*, Vol. 37, No. 8, 2004, pp. 2683–2685.

[4]. X. Yang, Z. Zhu, T. Dai, and Y. Lu, Facile fabrication of functional polypyrrole nanotubes via a reactive self-degraded template, *Macromol. Rapid Commun.*, Vol. 26, No. 21, 2005, pp. 1736–1740.

[5]. M. Li, W. Li, J. Liu, and J. Yao, Preparation and characterization of PPy with methyl orange as a soft template, *J. Mater. Sci. Mater. Electron.,* Vol. 24, No. 3, 2013, pp. 906–910.

[6]. Y. Li, P. Bober, M. Trchová, and J. Stejskal, Polypyrrole prepared in the presence of methyl orange and ethyl orange: Nanotubes versus globules in conductivity enhancement, *J. Mater. Chem. C,* Vol. 5, No. 17, 2017, pp. 4236–4245.

[7]. A. Chowdhuri, P. Sharma, V. Gupta, K. Sreenivas, and K. V. Rao, $H_2S$ gas sensing mechanism of $SnO_2$ films with ultrathin CuO dotted islands, *J. Appl. Phys.*, Vol. 92, No. 4, 2002, pp. 2172–2180.

[8]. A. T. Mane, S. T. Navale, S. Sen, D. K. Aswal, S. K. Gupta, and V. B. Patil, Nitrogen dioxide ($NO_2$) sensing performance of p-polypyrrole/n-tungsten oxide hybrid nanocomposites at room temperature, *Org. Electron.,* Vol. 16, No. 2, 2015, pp. 195–204.

[9]. N. Barsan, C. Simion, T. Heine, S. Pokhrel, and U. Weimar, Modeling of sensing and transduction for p-type semiconducting metal oxide-based gas sensors, *J. Electroceramics*, Vol. 25, No. 1, 2010, pp. 11–19.

[10]. P. Rai, C. Change, J. Yoon *et al.,* Design of highly sensitive and selective Au@NiO yolk–shell nanoreactors for gas sensor applications, *Nanoscale*, 6, 2014, pp. 8292-8299.

[11]. M. T. Ramesan and V. Santhi, Synthesis, characterization, conductivity, and sensor application study of polypyrrole/silver doped nickel oxide nanocomposites, *Compos. Interfaces*, Vol. 25, No. 8, 2018, pp. 725–741.

[12]. L. Pan, S. Ma, L. Li, and Y. Chen, Synthesis of Ag/NiO composite nanosheets and empty microspheres and their highly effective electrocatalytic properties, *J. Sol-Gel Sci. Technol.,* Vol. 72, No. 1, 2014, pp. 161–170.

[13]. M. Joulazadeh and A. H. Navarchian, Polypyrrole nanotubes versus nanofibers: A proposed mechanism for predicting the final morphology, *Synth. Met.,* Vol. 199, 2015, pp. 37–44.

[14]. H. S. Abdulla and A. I. Abbo, Optical and electrical properties of thin films of polyaniline and polypyrrole, *Int. J. Electrochem. Sci.,* Vol. 7, No. 11, 2012, pp. 10666–10678.

[15]. H. Yoon, M. Chang, and J. Jang, Sensing behaviors of polypyrrole nanotubes prepared in reverse microemulsions: Effects of transducer size and transduction mechanism, *J. Phys. Chem. B,* Vol. 110, No. 29, 2006, pp. 14074–14077.

[16]. G. Li, C. Martinez, and S. Semancik, Controlled Electrophoretic Patterning of Polyaniline from a *Colloidal Suspension,* No. 20, 2005, pp. 4903–4909.

[17]. D. M. Nerkar, S. E. Jaware, and G. G. Padhye, Fabrication of a Novel Flexible Room Temperature Hydrogen Sulfide (H2S) Gas Sensor based on Polypyrrole Films, *Int. J. Sci. Res.,* Vol. 5, No. 3, 2016, pp. 106–111.

[18]. J. Škodová *et al.*, Polypyrrole-silver composites prepared by the reduction of silver ions with polypyrrole nanotubes, *Polym. Chem.,* Vol. 4, No. 12, 2013, pp. 3610–3616.

[19]. N. Pickup, J. Shapiro, and D, Wong, Extraction of Mercury and Silver into Base- Acid Treated PolyPyrrole Films: A possible Pollution Control Technology, *J. Polymer Research,* Vol. 8, No. 3, 2001, pp. 151-157.

[20]. N. Maráková *et al.,* Antimicrobial activity and cytotoxicity of cotton fabric coated with conducting polymers, polyaniline or polypyrrole, and with deposited silver nanoparticles, *Appl. Surf. Sci.*, Vol. 396, November 2017, pp. 169–176.

[21]. R. Garg, V. Kumar, D. Kumar, and S. K. Chakravarti, Polypyrrole Microwires as Toxic Gas Sensors for Ammonia and Hydrogen Sulphide, *J. Sensors Instrum.,* Vol. 3, No. 1, January 2015, pp. 1-13.

[22]. S. A. Waghuley, Tin Dioxide/Polypyrrole Multilayer Chemiresistor as a Hydrogen Sulfide Gas Sensor, *J. Electron Devices,* Vol. 10, 2011, pp. 433–437.

[23]. F. Carone Fabiani, G. Fratesi, and G. P. Brivio, Adsorption of $H_2S$, HS, S, and H on a stepped Fe(310) surface, *Eur. Phys. J. B,* Vol. 78, No. 4, 2010, pp. 455–460.


---